The 2009 IEEE/RSJ International Conference on
Intelligent Robots and Systems
October 11-15, 2009 St. Louis, USA

Safe Human Robot Interaction via Energy regulation control

Matteo Laffranchi[1,2], N. G. Tsagarakis[1] and Darwin G. Caldwell[1]

[1]Istituto Italiano di Tecnologia (IIT), Genova 16163, Italy

[2]The University of Sheffield, Western Bank Sheffield, S10 2TN, UK

Abstract— **This paper presents an energy-based control strategy to be used in robotic systems working closely or cooperating with humans. The presented method bounds the dangerous behavior of the robot during the first instants of the impact by limiting the energy stored into the system to a maximum imposed value.Two critical physical human robot interaction (pHRI) cases are studied, these are the collision either against a free or a clamped head. Safe energy values that can be used as reference were retrieved by analysing experimental data of energy absorption to failure of cranium bones and cervical spinal cords.The energy regulation control is implemented in a series elastic actuator prototype joint. The model and the control scheme of the system are analysed. The proposed control scheme is a position-based controller that adjusts the position trajectory reference in function of the maximum energy value imposed by the user. Preliminary results are presented to show that the actuator unit and this control scheme are capable of limiting the energy to a maximum imposed value.**

I. Introduction

In recent years the exploitation of robots within the human environment have rapidly increased. From the safety perspective this places new demands on the development of the robotic systems. Among others the actuation and the control strategy are probably the predominant factors that determine the overall safety index of the robotic machine.

Typical rigid manipulators employ a stiff connection between the motor and the link that makes the high frequency output impedance to be dominated by the sum of the link and the reflected rotor inertia. The latter term is often high due to the high gear ratio, making the robot to be unsafe during impacts. In order to overcome this problem, various safe-oriented control techniques have been developed for reducing the output impedance of the system [1], [2]. Unfortunately, these strategies are effective for frequencies that are below the closed loop bandwidth of the control system.

Matteo Laffranchi is with the Italian institute of Technology (IIT), Genova 16163, Italy (phone: +39 010 71781 418; e-mail: matteo.laffranchi@ iit.it), and within the University of Sheffield, Sheffield S10 2TN, UK.
Nikolaos G. Tsagarakis is with the Italian institute of Technology (IIT), Genova 16163, Italy (phone: +39 010 71781 428; e-mail: nikos.tsagarakis@ iit.it).
Darwin G.Caldwell is with the Italian institute of Technology (IIT), Genova 16163, Italy (e-mail: darwin.caldwell@ iit.it).

In contrast to the "stiff" approach, a wide range of experimental novel compliant actuation systems [3], [4], [5], [6], [7] have been developed during the past fifteen years incorporating inherent safety mechanisms.

The series elastic actuator (SEA) family is an early development towards the realization of actuator units with intrinsic compliance. This family employs a fixed compliance element which decouples the output of the high impedance actuator from the load. Some examples of the SEA can be found in [5], [6], [7], [8]. The main advantage of a SEA system is that, by mechanically decoupling the link from the rotor, it makes the output impedance to be low across the frequency spectrum. At frequencies below the closed loop bandwidth of the SEA control, the output impedance can be further tuned via control laws, while at high frequencies (e.g. during the first stage of a blunt impact), the elasticity of the joint mechanically decouples the output link from the rotor, making the output impedance to be dominated by the link inertia. Thus, by means of an appropriate mechanical structure (e.g. SEA design) and a safe-oriented control strategy, the typical problem of the safety of rigid torque controlled robotic systems over the frequency spectrum can be addressed.

The safety of a robotic structure is often characterized by means of safety indexes which were developed in fields that are different from robotics. A well known safety criterion is the Head Injury Criterion, or HIC [9] which was born in the automotive industry and has been used in [5], [10-13]. These indexes are based on tests that emulate collisions where the orders of magnitude of the physical variables (e.g. velocity) are significantly different from those of a generic robotic system. In addition, the computation of this index uses only the acceleration of the head during the impact, without taking into account the sequence of events and the boundary conditions. For instance, it does not distinguish between the case of a collision with a free head or a collision with a clamped head, despite the fact that the risks are very different for the two cases [13]. It is clear from the above that these criteria are not suited to characterize the safety of a robotic system. In addition, as far as the HIC is concerned, the complexity and the computation requirements of this index make difficult the real time implementation of this criterion within the control system of a robotic device in order to ensure safety. To calculate the HIC index it is necessary to have a model of the head, to simulate the impact between the robot and the head, and then integrate

the retrieved acceleration of the head in the time domain between the two time extremes that maximize the index during the impact phase.

In this paper a new concept to measure and control the safety of a robotic structure that takes into account the physical characteristics of the system e.g. the inertia and the joint stiffness is presented. Furthermore, making the robot always work in a safe region, this control strategy prevents the danger that can be caused by collision instead of counteracting only after the collision is detected. The proposed control method is implemented and evaluated on a prototype series elastic robotic joint. The paper is structured as follows: Section II presents the critical human-robot collision scenarios considered in this work and reports on the energy exchange safety limits. The dynamic model of a series elastic actuation unit and the energy regulation control are introduced in section III, while in section IV, experimental results validate the proposed control strategy. Finally, section V addresses the conclusions and future work.

II. CRITICAL HUMAN-ROBOT COLLISIONS - SAFE ABSORBED ENERGY MARGINS

A. Critical Human-robot collision scenarios

In this study, the collision between the robot and the human head is considered as a reference case since the head is one of the most delicate parts of the human body. Two collision cases are analyzed. In the first case, Figure 1a, the robot is colliding against a clamped head, while in the second case the robot is colliding against a head that can accelerate after the collision with the robot link. These two cases have been already analyzed in [12], [13], where an evaluation of the potential severity of the impacts by means of safety indexes is provided.

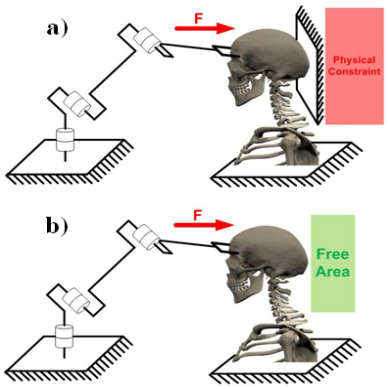

Fig. 1 Clamped head (a) and Free head (b) collision case

In the first case the impact forces are only exerted on the skull bones, while in the second case, after the first stage of the impact, the head can be subject of high acceleration /velocity motion exerting stress on the neck that can be equally or more significant than the stress exerted on the skull bones. In the first case the energy absorbed by the human cranial bone is examined, while for the second case it is useful to take also into consideration the energy absorbed by the human upper cervical bone.

B. Clamped head case - Safe absorbed energy levels for the Cranial bone

Data on the amount of energy required to cause the failure of the cranial bones can be found in [14], [15]. One interesting aspect of the results obtained in these studies is that, even if the mechanical properties (e.g. elastic modulus) of the bone and the suture of the skull are different, the amount of energy required to cause the failure is approximately the same for both structures [14]. In [15] skulls of adult humans were exposed to dynamic tests with stress rates ranging from 0.005sec^{-1} to 150sec^{-1}. The results show that the energy absorbed to failure is constant over the spectrum while the modulus of elasticity, the breaking stress and the breaking strain depend on the excitation rate [15]. The above suggests that shaping the energy level of the robotic device can be a suitable strategy which can guarantee low accidental risks during collisions between the robot and the human. From [15] the linear regression of the values of energy absorbed to failure measured in 120 specimens over the spectrum returns an energy/volume ratio of $\varepsilon_{failure\_adult} \approx 0.29 \frac{N \cdot mm}{mm^3}$.

The volume of the head can be computed using the following formula from [16]:

$$V_{adult\_head} \approx 0.5238 \cdot L \cdot B \cdot H \qquad (1)$$

Where L is the maximum antero-posterior length of the skull, B is the breadth and H is the height. For the typical adult skull $L = 196mm$, $B = 155mm$, $H = 112mm$ [17]. By multiplying (1) with the energy/volume ratio the energy level that can cause the failure of a typical adult skull can be derived to be equal to:

$$\varepsilon_{ABS\_failure\_adult} = \varepsilon_{failure\_adult} \cdot V_{adult\_head} \approx 517J \qquad (2)$$

The above energy level is just an indicative value of the energy required to break a typical adult human skull. In this work a more conservative level is considered in order to prevent not only the failure of the skull bone but also to minimize the risk of a serious injury. Such a conservative level can be the energy required to produce the same effects on an infant human head instead of an adult human head. In contrast to the stiff adult cranium, the infant skull is a compliant structure capable of substantial deformation under external loading and is thus much more delicate. In [14] experiments were carried out to check the rupture of the three-point bending at two velocity rates: in a first case a quasi-static excitation is forced on the cranium with the velocity of the loading nose equal to 2.5mm/min ($42.3 \cdot 10^{-6}$ m/s), while in the second case the loading nose is moving at a velocity that is 2540mm/min ($42.3 \cdot 10^{-3}$ m/s). In the case of the "slow" loading nose the amount of energy absorbed is smaller if compared with the other case. In contradiction to

the human adult cranium case, the absorption of energy to failure is a function of the strain rate and, of course, of the age of the infant (Fig. 2).

As expected, the energy absorbed to failure in this case is smaller than that of the adult human head and equal to $\varepsilon_{failure\_child} \approx 0.16 \frac{N \cdot mm}{mm^3}$. This is the mean value of the results obtained from specimens of 6 months old infants [14], see Fig.2.

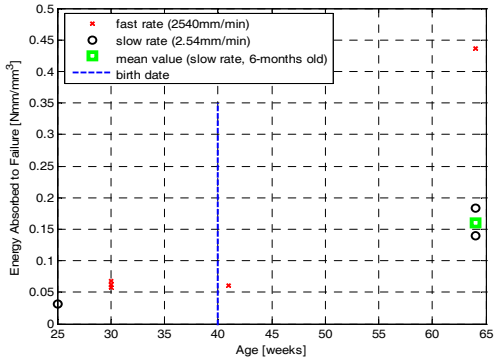

Fig. 2 Energy absorbed to failure versus age – human cranial bone in three point bending [14]

The typical volume of infant skulls can be found in [18]. For a 6-months old infant this is equal to:

$$V_{child\_head} \approx 750 \cdot 10^3 mm^3 \quad (3)$$

Therefore, the level of energy that can cause the failure of a typical 6 months old child skull is equal to:

$$\varepsilon_{ABS\_failure\_child} = \varepsilon_{failure\_child} \cdot V_{head\_child} \approx 120\ J \quad (4)$$

It is reasonably lower compared with the one shown in (2) and, thus, far from the dangerous energy levels required to seriously injure the cranium of an adult human being.

C. *Unclamped case - Safe absorbed energy level for the neck*

Injuries to the cervical spinal cord are of special concern, because damage in this region may result in deficits ranging from slight motor and sensory losses in the lower limbs to complete quadriplegia and lifelong ventilator dependency.

In [19] it has been shown that, during normal human head motion, quite large axial strains occur in the cervical spinal cord, although these probably occur at low and not dangerous strain rates. However, during accidental sudden impacts strains in the spinal cord occur very rapidly, resulting in temporary or permanent loss of neural function that is closed to the injured region. Measures of the level of the absorbed energy that may cause the failure of the cervical spinal cord can be found in [20]. An average value for this parameter experimentally estimated using 7 intact adult specimens is

$$\varepsilon_{mean\_neck} \approx 30J \quad (5)$$

The value in (5) represents a mean energy value which takes into account different kinds of pathologies, from the disruption of ligaments to the fracture of certain bones of the cervical spinal cord. It can be noticed that this value is much smaller than those in (2) and (4). This implies that from the energy absorption and failure point of view, the neck is a much more delicate structure compared to the cranial bone.

Table 1, below, summarizes the minimum absorbed energy levels, which may cause critical injuries in a human head or neck, during accidental collision of the clamped or free human head with a robot.

TABLE I
VALUES OF SAFE ABSORBED ENERGY MARGINS

Case	Analyzed structure	Energy [J]
Clamped case	Adult cranium	517
	6-months old infant cranium	120
Unclamped case	Adult neck	30

III. ENERGY REGULATION CONTROL

The basic concept of this control strategy is to limit the energy stored into the structure of the robot (joint and link) in safe levels below those introduced in section II. During the accidental collision the worst case condition is assumed, that is, all the energy stored in the link is transferred to the collided body.

A. *The series elastic actuation prototype unit*

The proposed energy regulation control was implemented and evaluated on a single SEA joint. The actuator used consists of three main components: a typical brushless DC motor, a harmonic reduction drive and the rotary passive compliant module.

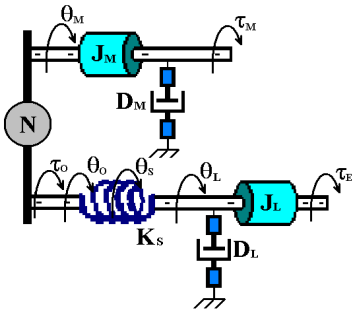

Fig. 3 Compact SEA mechanical model diagram

These three components can be represented by the mechanical model shown in Fig. 3. The model is composed of the rotary inertia and viscous damping of the motor J_M, D_M, the gear drive with the reduction ratio of N, the elastic module with an equivalent spring constant of K_s, the output link inertia and axial damping coefficient J_L, D_L. In addition, θ_M, θ_O are the motor mechanical angles before and after the reduction drive, θ_L is the angle of the output

link and θ_S is the rotary defection of the elastic module with respect to θ_O such as that

$$\theta_L = \theta_O + \theta_S \tag{6}$$

Finally, τ_M is the torque provided by the actuator while τ_O is the input torque of the elastic element and τ_E is the torque applied to the system by the load and/or the environment. The above system can be described by the following set of dynamic equations.

$$(J_M \cdot N^2 \cdot s^2 + D_M \cdot N^2 \cdot s + K_S) \cdot \theta_O - K_S \cdot \theta_L = \tau_O \tag{7}$$

$$(J_L \cdot s^2 + D_L \cdot s + K_S) \cdot \theta_L - K_S \cdot \theta_O = \tau_E \tag{8}$$

B. Trajectory shaping based on energy regulation control

Consider now the scenario of the single joint robotic system, based on the actuation unit of Fig.3, interacting with the body of the human operator, as depicted in Fig.4. The amount of energy stored by the generic robot link body shown in Fig. 4 is given by:

$$\varepsilon_{tot} = \varepsilon_k + \varepsilon_e + \varepsilon_g \tag{9}$$

Where ε_k is the translational and rotational kinetic energy, ε_e is the elastic potential energy and ε_g is the gravitational potential energy. The energy stored into the prototype link as function of the parameters of the joint model introduced in Fig. 3 is given by

$$\begin{aligned} \varepsilon_{tot} &= \frac{1}{2} K_S \cdot \theta_S^{\,2} + \frac{1}{2} J_L \cdot \left(\dot{\theta}_0 + \dot{\theta}_S\right)^2 + \\ &+ \frac{1}{2} J_M \cdot \left(\dot{\theta}_0 \cdot N\right)^2 + \frac{1}{2} m_L \cdot \left[\left(\dot{\theta}_0 + \dot{\theta}_s\right) \cdot l_{COG}\right]^2 + \\ &+ m_L \cdot g \cdot \sin(\theta_0 + \theta_S) \cdot l_{COG} \end{aligned} \tag{10}$$

Where the additional parameters introduced are the mass of the link m_L, the acceleration of gravity g and the distance between the axis of rotation and the center of gravity of the link l_{COG}. Applying a limit on this energy results in

$$\varepsilon_{tot} < \varepsilon_{\max} \tag{11}$$

From the above energy limit $\varepsilon_{\max}$ the limit of the spring deflection angle θ_s can be derived from (10) given the instantaneous kinetic and gravitational energy of the link.

$$\theta_{SMAX}(t) = \pm \sqrt{\frac{\left(\varepsilon_{\max} - \varepsilon_k(t) - \varepsilon_g(t)\right) \cdot 2}{K_S}} \tag{12}$$

However, (12) gives a solution only if the term under the square root is bigger than zero, i.e. when the total energy stored is dominated by the elastic potential energy, which is the case of unexpected collision or interaction with the environment. The term under the square root is negative when the sum of the kinetic and the gravitational potential energy is greater than the maximum energy allowed. Assuming that the robot manipulator is designed for safety, the maximum gravitational potential energy stored would be much smaller than the maximum energy threshold, and thus the condition in which the term becomes negative would be when the total energy stored is dominated by the kinetic energy, which is the case of a free motion at a velocity that makes the kinetic energy to reach the energy threshold ε_{max}. In this case, a term $\Delta\theta_0$ is used to generate a new reference angle (see equation (14)) given the current angle θ_0:

$$\Delta\theta_0(t) = \pm \sqrt{\frac{-\left(\varepsilon_{\max} - \varepsilon_k(t) - \varepsilon_g(t)\right) \cdot 2}{K_S}} \tag{13}$$

The sign of the terms in (12) and (13) is determined by the conditions reported in Tab. II, where the case of possible interaction is distinguished by the following condition: $\varepsilon_e > \varepsilon_{\max} - \varepsilon_k - \varepsilon_g > 0$; while the situation of possible free motion is detected by $\varepsilon_{\max} - \varepsilon_k - \varepsilon_g < 0$.

TABLE II
POSSIBLE WORKING CONDITIONS

POSSIBLE INTERACTION	$\theta_S > 0 \Rightarrow \theta_{SMAX} > 0$
	$\theta_S < 0 \Rightarrow \theta_{SMAX} < 0$
POSSIBLE FREE MOTION	$\dot{\theta}_0 > 0 \Rightarrow \Delta\theta_0 < 0$
	$\dot{\theta}_0 < 0 \Rightarrow \Delta\theta_0 > 0$

Given the maximum allowable energy the objective of the control strategy is to adjust the reference trajectory of the joint when the energy stored in the link exceeds the maximum limit imposed. When this condition is verified the trajectory is adjusted in order to ensure that the deflection does not become bigger than the maximum allowed preventing the energy levels from exceeding the preset safe value.

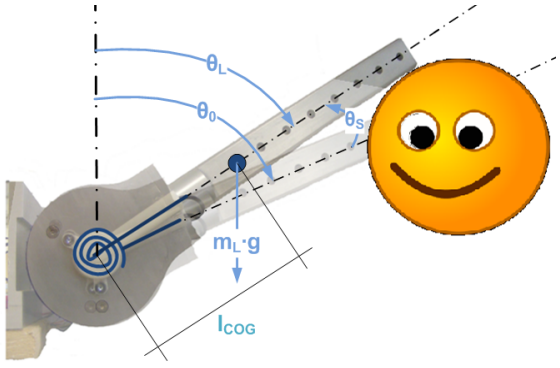

Fig. 4 Compliant actuator configuration

To achieve the above the trajectory modification module uses a proportional control law to regulate the reference trajectory. In particular, during the interaction the trajectory regulation law uses the difference between the instantaneous spring deflection angle θ_s and the maximum deflection angle θ_{SMAX} given by (12). For the free motion case the correction term of (13) is used to compute the modified

reference trajectory of the joint θ_{OD_MOD} from the measured angle θ_O.

The combined trajectory regulation law for both cases can be expressed as follows:

$$\theta_{OD\_MOD}=\begin{cases}\theta_{OD};\varepsilon_{tot}<\varepsilon_{\max}\\ \theta_O+(\theta_S-\theta_{SMAX})\cdot K_{p\_INT};\varepsilon_e>\varepsilon_{\max}-\varepsilon_k-\varepsilon_g>0\\ \theta_O+\Delta\theta_0\cdot K_{p\_FM};\varepsilon_{\max}-\varepsilon_k-\varepsilon_g<0\end{cases} \quad (14)$$

Where the term K_{p_INT} is the proportional gain used for the interaction case and K_{p_FM} is the proportional gain used for the free motion case. When the total energy stored exceeds the maximum allowed, the control system switches the value of the reference angle θ_{OD} to the modified one in function of the detected condition, according to (14). When the total energy stored is lower or equal than the maximum allowed, the system switches back to the reference value of the desired trajectory angle θ_{OD}. A representation of the energy regulation control strategy is illustrated in Fig. 5. To prevent the high frequency components, introduced by the switching between reference trajectory and the safety imposed value, from entering the servo loop, a weighted mean between the desired trajectory angle θ_{OD} and the modified reference trajectory of the joint θ_{OD_MOD} was implemented.

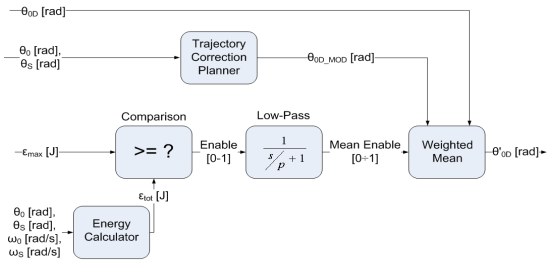

Fig. 5.The trajectory modification module of the energy regulation control scheme

The signal "Enable" is the switching signal generated from the results of the comparison between the total energy stored, ε_{tot} and the maximum energy threshold $\varepsilon_{\max}$. This signal, is low-pass filtered to give ME (Mean Enable), which is used as a weight for the "Weighted mean" block. . The filter in Fig.5 is an adaptive first order filter, being its bandwidth set in function of the difference between θ_{OD} and θ_{OD_MOD}. In detail, the pole of this filter is set to $p=\dot{\theta}_{0MAX}\cdot|(\theta_{0D}-\theta_{0D\_MOD})^{-1}|$. In this way, the maximum value of the derivative of the position reference (velocity) is limited to a maximum value $\dot{\theta}_{0MAX}$ obtained from a safety-based criterion (in this case, $\dot{\theta}_{0MAX}$ is the velocity that makes the kinetic energy to reach the maximum allowed ε_{MAX}). This makes the controller to not to inject large magnitude commands that can result unsafe during transitions from θ_{OD} to θ_{OD_MOD} and vice versa. The signal θ'_{0D} is the output of the block "Weighted Mean" and is given by

$$\theta'_{0D}(t)=ME(t)\cdot\theta_{0D}(t)+(1-ME(t))\cdot\theta_{0D\_MOD}(t) \quad (15)$$

The overall energy regulation control scheme is shown in Fig. 6.

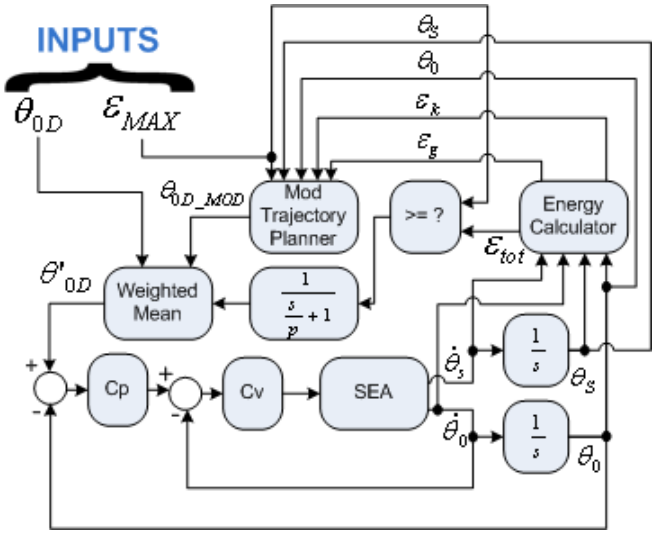

Fig. 6 Block scheme of the energy regulation control

IV. Experimental Results

Experiments were conducted in order to verify the performance of the energy regulation control scheme introduced in the previous sections. The experiments were performed using the prototype actuation unit [6] shown in Fig. 7.

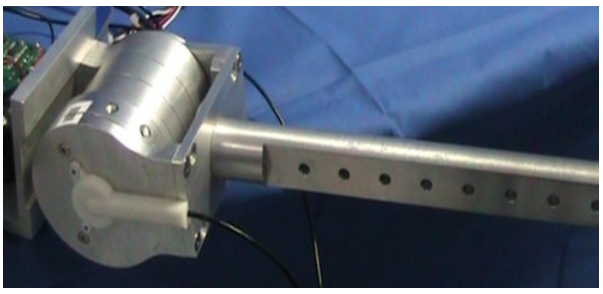

Fig. 7 Free motion case test setup

Two potentially risky cases were analyzed: the case of an accidental collision, and a case of free motion at a high velocity. For both cases the highest contribution on the energy stored into the joint is given either by the elastic potential energy or the kinetic energy. The gravitational potential energy is not giving a relevant contribution to the overall energy, this is because this system has a lightweight link (m_L = 0.41 kg) giving a maximum value of $\varepsilon_{g\_max} \approx 0.45J$.

A. *Accidental collision case*

In these trials the motor was commanded to follow a sinusoidal trajectory while collisions were generated within the range of motion of the link using a soft obstacle made of foam, Fig. 8.

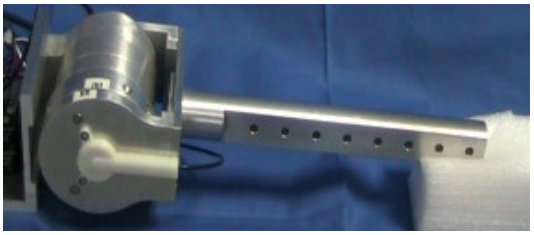

Fig. 8 Accidental collision test setup

The trajectory parameters and the energy limit applied are illustrated in Table III. The maximum energy imposed was set equal to 0.8J, which is much smaller than the values shown in Table I. This was done in purpose in order to test the behavior of the control system avoiding big force-torque exchanges that can damage the test equipment.

TABLE III
MOTION/ENERGY PARAMETERS OF THE COLLISION EXPERIMENT

Parameter	Value
Amplitude of the trajectory reference A	0.7 rad
Frequency of the trajectory reference ω	0.25Hz
Maximum energy value imposed ε_{max}	0.8 J

Fig. 9a depicts the trends of the energy components.

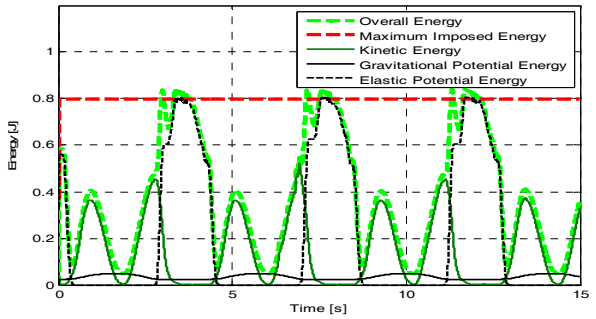

(a)

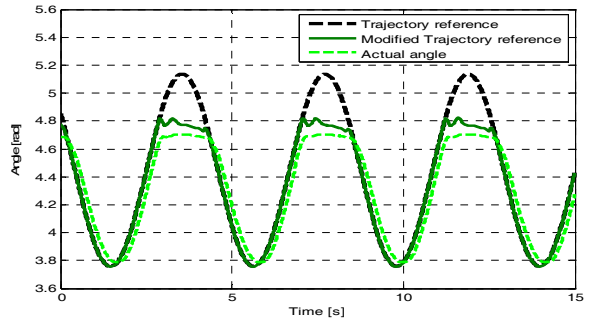

(b)

Fig. 9 Impact case: a) Energy components b) Trajectory modification

It can be observed that during the impact, the kinetic energy drops to zero as a consequence of the decrease of the velocity of the link. The potential energy grows accordingly with the spring deflection due to the impact, making the overall energy to exceed the maximum allowable value. In this case the control works to limit the elastic potential energy, because the kinetic energy and the gravitational potential energy are constant due to the fact that the link is not in motion. Fig. 9b depicts how the trajectory angle is modified in order to achieve the goal.

B. *Free motion case*

In the second experiment the joint performed a free motion driven by a sinusoidal trajectory with the parameters shown in Table IV. The parameters of the reference trajectory were selected in order to make the system exceed the maximum energy in order to demonstrate the control action.

TABLE IV
MOTION AND ENERGY PARAMETERS OF THE FREE MOTION EXPERIMENT

Parameter	Value
Amplitude of the trajectory reference A	0.92 rad
Frequency of the trajectory reference ω	0.32Hz
Maximum energy value imposed ε_{max}	0.8 J

In this case, apart from the gravitational potential energy that is very small due to the light weight link, the elastic potential energy is also close to zero since the deflection of the spring is minimum during the free motion due to the high stiffness-link inertia ratio ($K_S = 190 Nm \cdot rad^{-1}$; $J_L = 4.98 \cdot 10^{-3} kg \cdot m^2$). Therefore the overall energy is determined by the kinetic energy. Fig.10a shows the energy components of the joint.

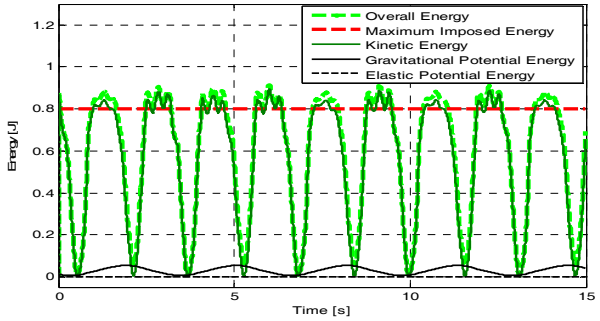

(a)

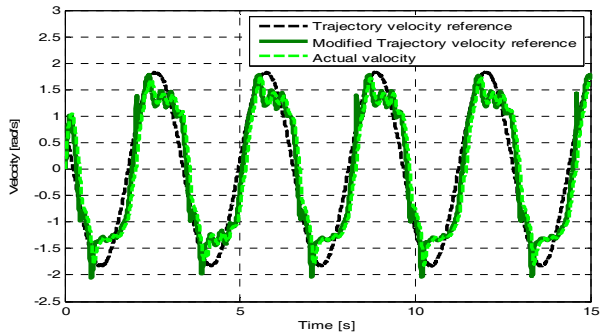

(b)

Fig. 10 Free motion case: a) Energy components b) Trajectory modification

As expected the overall energy is very close to the kinetic energy. In Fig. 10b it can be seen how the link velocity trajectory is limited in order to constrain the total energy of the system within the maximum set value. As the trajectory velocity exceeds 1.5 rad/s the control adjusts the reference in order to limit the total energy. As the trajectory velocity becomes smaller than the 1.5 rad/s threshold the reference velocity trajectory is tracked again.

V. CONCLUSIONS AND FUTURE WORK

In this paper a safe-oriented strategy to control a SEA system was presented. By combing the series elastic mechanical design and the energy regulation control a strategy to face the problem of the safety during the first instants of the impact, (i.e. the problem occurring in rigid torque-controlled robots) is proposed. The specific case presented here can be extended to a generic elastic joint as well as to multi-DOF systems.

The technique presented constrains the energy stored into the robotic link to a maximum value that can be derived by a safety criterion. The proposed control scheme is a position based controller that adjusts the trajectory reference position as a function of the desired maximum energy value using the states of the system. The overall system was experimentally evaluated using a prototype SEA unit.

Future developments will include the implementation of this concept in a robotic arm. The manipulator on which this method will be tested has to be designed following safe-oriented criteria (e.g. soft and lightweight): this will allow lower amounts of energy storage which would be well below the maximum energy threshold during the execution of normal operations. In such a case, performance will not be limited. The arm described will be then used to validate thoroughly the system safety level. Further work will be done on the frequency-domain characterization and the stability analysis of the energy based safe control.

ACKNOWLEDGMENT

This work is supported by the VIACTORS, FP7-ICT-2007-3 European project.

REFERENCES

[1] N. Hogan. “Impedance control: An approach to manipulation, part I - theory, part II - implementation, part III – applications” Journ. of Dyn. Systems, Measurement and Control, 107:1-24, 1985.

[2] A. De Luca, A. Albu-Schaeffer, S. Haddadin, G.Hirzinger, “Collision detection and safe reaction with the DLR-III lightweight manipulator arm” IEEE/RSJ International Conference on Intelligent Robots and System, Beijing, China, Oct 2006

[3] G. Tonietti, R. Schiavi, and A. Bicchi, “Design and Control of a Variable Stiffness Actuator for Safe and Fast Physical Human/Robot Interaction”, IEEE International Conference on Robotics and Automation, Barcelona, Spain, April 2005.

[4] R. Schiavi, G. Grioli, S. Sen, A. Bicchi, “VSA-II: a Novel Prototype of Variable Stiffness Actuator for Safe and Performing Robots Interacting with Humans”, in 2008 IEEE International Conference on Robotics and Automation Pasadena, CA, USA, May 19-23, 2008

[5] M. Zinn, O. Khatib, and B. Roth, “A new actuation approach for human friendly robot design”, The international journal of robotics research, Vol. 23, No.4-5, April-May 2004, pp. 379-398

[6] N.G. Tsagarakis, M. Laffranchi, B. Vanderborght and D.G. Caldwell, “A Compact Soft Actuator Unit for Small Scale Human Friendly Robots”, 2009 IEEE International Conference on Robotics and Automation Kobe, Japan, May 2009, (accepted).

[7] Pratt G. and Williamson M., “Series elastic actuators”, Proceedings of IEEE/RSJ International Conference on Intelligent Robots and Systems, 1995, vol. 1, pp. 399–406.

[8] J. Pratt and G. Pratt, “Intuitive control of a planar bipedal walking robot", International Conference on Intelligent Robots and Systems, 1998.

[9] J. Versace, “A Review of the severity index”, in Proc. 15th Stapp Car Crash Conference, 1971, New York, pp. 771-796.

[10] A. Bicchi, G. Tonietti, “Fast and “Soft-Arm” Tactics”, IEEE Robotics and Automation Magazine, 11 (2), 12-21.

[11] S. Haddadin, A. Albu-Shaeffer, G. Hirzinger, “Safety Evaluation of Physical Human-Robot Interaction via Crash-Testing”, Robotics: Science and Systems Conference (RSS 2007)

[12] S. Haddadin, A. Albu-Schaeffer and G.Hirzinger, “The Role of the Robot Mass and Velocity in Physical Human-Robot Interaction - Part I: Non- Constrained Blunt Impacts”, IEEE International Conference on Robotics and Automation, Pasadena, CA , USA, May 19-23, 2008

[13] S. Haddadin, A. Albu-Schaeffer, M. Frommberger and G.Hirzinger, “The Role of the Robot Mass and Velocity in Physical Human-Robot Interaction - Part II: Constrained Blunt Impacts”, IEEE International Conference on Robotics and Automation, Pasadena, CA , USA, May 19-23, 2008

[14] S.S. Margulies, K.L. Thibault, “Infant Skull and Suture Properties: Measurements and Implications for Mechanisms of Pediatric Brain Injury”, J. Biomech. Eng. August 2000 - Vol. 122

[15] J.L. Wood, “Dynamic Response of Human Cranial Bone”, J. Biomechanics, Vol 4, Pergamon Press, 1971

[16] K.Y. Manjuath, “Estimation of Cranial Volume – an Overview of Methodologies”, J. Anat. Soc, India 2002

[17] A.R. Tilley, H.D. Associates, “The Measure of Man and Woman: Human Factors in Design”, Whitney Library of Design, 1993

[18] S. Sgouros, H. Goldin, A. Hockley, M. Wake, K. Natarajan, “Intercranial volume change in childhood”, Journal of Neurosurgery, 91, 1999

[19] L. E. Bilston and L. E. Thibault, “The Mechanical Properties of the Human Cervical Spinal Cord In Vitro”, Annals of Biomedical Engineering, Vol 24, pp. 67-74, 1996

[20] Yogananandan, N. et al, “Human head-neck biomechanics under axial tension”, Med. Eng. Phys., Vol 18, N° 4, pp 289-294, 1996 Elsevier Science Ltd.